Original Article

Quantitative proteomics reveals specific protein regulation of severe hypospadias

Shibo Zhu, Wen Fu, Jinhua Hu, Xiangliang Tang, Yanhong Cui, Wei Jia

Department of Pediatric Urology, Provincial Key Laboratory of Research in Structure Birth Defect Disease, Guangzhou Women and Children's Medical Center, Guangzhou Medical University, Guangzhou, China

Contributions: (I) Conception and design: S Zhu; (II) Administrative support: W Fu, W Jia; (III) Provision of study materials or patients: J Hu, X Tang, Y Cui; (IV) Collection and assembly of data: S Zhu; (V) Data analysis and interpretation: S Zhu; (VI) Manuscript writing: All authors; (VII) Final approval of manuscript: All authors.

Correspondence to: Wei Jia. Department of Pediatric Urology, Guangzhou Women and Children's Medical Center, Guangzhou Medical University, Guangzhou, China. Email: jiawei198044@hotmail.com.

Background: The etiological mechanism of hypospadias is multifactorial and may be heterogeneous by severity. To date, very limited analyses on proteome in hypospadias have been conducted, and there are still no severe hypospadias proteomics analyses.

Methods: In our study, tandem mass tag (TMT)-based quantitative proteomics was performed, exploring the clinical samples from hypospadias patients and healthy donators, in order to identify distinctly expressed proteins for severe hypospadias. To further uncover the mechanistic links in these complex proteomics data, we performed several core ingenuity pathway analyses (IPA) to predict, based on these observed different expression of proteins (DEPs).

Results: Compared with the unaffected controls, 299 proteins were found to be down-regulated and 176 proteins up-regulated in severe hypospadias foreskin tissues. Functional annotation revealed that these DEPs were mainly in the extracellular space and were associated with complement activation and coagulation cascades. Similarly, the IPA core analysis revealed enriched pathways of the acute phase response signaling and complement system, demonstrating that by mediating their targeted, differentiated expressed proteins (A2M, APOE, C4A/C4B, C5, CAT, CD74, CFP, CREB1, CTSB, FGA, FGB, FGG, FN1, FOS, HP, LYZ, PF4, RBP1, S100A12, SERPINA3, SLC2A1, and THBS1) may be involved in the activation of myeloid cell degranulation, phagocytes degranulation, molecule secretion, and were mainly regulated by CSF1, JNK, STAT1, and STAT3.

Conclusions: Our findings raise questions regarding the role of inflammatory activity in the pathology of severe hypospadias. This approach highlights the possibility of the use of non-surgical approaches to limit fibrotic signals and function, which is a promising potential therapeutic strategy for hypospadias patients.

Keywords: Quantitative proteomics; severe hypospadias; complement activation; fibrosis

Submitted Feb 16, 2022. Accepted for publication Apr 18, 2022.
doi: 10.21037/tau-22-155
View this article at: https://dx.doi.org/10.21037/tau-22-155

Introduction

Hypospadias, the second most common congenital anomaly in newborn males (1), is a birth defect in which the urethral opening is proximally displaced along the ventral side of the penis rather than at tip of the penis (2). Severe hypospadias, accounting for 30% of total hypospadias cases, are defined as posterior position of the urethral opening ranging from proximal penile to perineal and intimately associated with higher degree of penis curvature (chordee) resulting from extensive fibrous tissue, dartos tethering and a short urethral plate (3,4). Clinically, compared with mild type, it's been

a persisting challenge due to its rising prevalence over the last two decades, multi-stage surgeries requirement, higher rates of complication such as recurrent stenosis or fistulae and poorer long-term outcomes (5).

The etiological mechanism of hypospadias is multifactorial and heterogeneous by severity (6,7). Previous studies have suggested the role of genetic heritability, focusing on genes related to androgens (e.g., androgen receptor, AR), oestrogens and oestrogen-responsive genes (e.g., cyclic ANP-dependent transcription factor, ATF3) (8), growth factors during development (e.g., homeobox protein Hox-A4 and Hox-B6, bone morphogenetic protein 4 and 7) (9), and transcription factors (e.g., Wilms tumour protein WT1). However, genetic hereditability only attributes to no more than <10% of hypospadias cases (10,11). The interplay roles of maternal metabolic traits (8,12), environmental exposures and epigenetic regulations (13,14) have also been highlighted. Given the numerous suspected roles, the etiology of hypospadias remains incompletely understood and it would be worthwhile to investigate the downstream products of genes (15).

Proteins, as the ultimate performer of biological functions, its alternations may more directly reflect the occurrence of disease. Benefiting from innovation in mass spectrometry (MS) and advances in peptide labelling, proteomics study enables the identification and quantification of changes in protein expression in the entire proteome. Recently, Piñeyro-Ruiz *et al.* created a proteomics landscape of mild hypospadias, which highlighted the proteomics characteristics of hypospadias and revealed changes with essential cellular processes related to energy production and apoptosis (16). However, to date, no severe hypospadias proteomics analyses have been introduced.

In our study, tandem mass tag (TMT)-based quantitative proteomics, which explores the clinical samples from hypospadias patients and healthy donors, was performed to identify distinctly expressed proteins for severe hypospadias. To further uncover the mechanistic links in these complex proteomics data, we performed several core ingenuity pathway analyses (IPA) to infer [based on these observed different expression of proteins (DEPs)]: (I) which pathways are changed and the directional effects on the pathway; (II) the regulatory effects of these DEPs, including the upstream regulators and the downstream effected cellular processes and biological functions; and (III) the associated interaction networks of these DEPs. We present the following article in accordance with the MDAR reporting checklist (available at https://tau.amegroups.com/article/view/10.21037/tau-22-155/rc).

Methods

Ethics statement

This study protocol was approved by the Ethics Committee of Guangzhou Women and Children's Medical Center, Guangdong, China (No. GWCMC-2020201), and was carried out in accordance with all relevant guidelines and regulations. Written informed consent was obtained from all patients or their parental/legal guardians. The study was conducted in accordance with the Declaration of Helsinki (as revised in 2013).

Patient samples

From February 2020 to June 2020, five boys with severe hypospadias who underwent first urethroplasty and five control group boys scheduled for elective circumcision at the Department of Pediatric Urology, GWCMC were recruited by simple randomization. Diagnosis of hypospadias and surgery were performed by a senior pediatric urologist with over 15 years of practice. Severe hypospadias was defined as urethral opening displaced at subcoronal, penile shaft, scrotal, and perineal areas, accompanied by chordee. Clinical information, including age at surgery and urethral opening location, was collected.

Protein extraction, digestion, and TMT labeling

Surgical-resected preputial specimens of these subjects were preserved in liquid nitrogen immediately after harvesting in the operation room and stored at −80 ℃ until use. Minced foreskin tissues were lysed in SDT buffer (4% SDS, 100 mM Tris-HCl, pH7.6). The lysate was homogenized using a MP Fastprep-24 Automated Homogenizer (24×2, 6.0 M/S, 60 s, twice), sonicated, boiled for 10 min, and centrifuged at 14,000 g for 40 min. The BCA assay kit (P0012, Beyotime, Shanghai, China) was used to determine the concentration of proteins. The proteins were separated on 12.5% SDS-PAGE. Then, 200 μg of protein of each sample was digested according to the filter aided sample preparation (FASP) procedure; 100 μg peptide mixture of each sample were labeled using TMT 10-plex kits (Thermo Fisher Scientific, Rockford, USA) according to the

manufacturer's instructions.

Peptide fractionation with reversed phase (RP) chromatography

TMT-labeled peptides were fractionated by RP chromatography using the Agilent 1260 infinity II HPLC. The peptide mixture was diluted with buffer A (10 mM HCOONH4, 5% ACN, pH 10.0), loaded onto a XBridge Peptide BEH C18 Column, 130Å, 5 µm, 4.6 mm × 100 mm column and eluted at a flow rate of 1 mL/min with gradient. The elution was monitored by measuring absorbance at 214 nm. Fractions were collected every 1 min during 31–65 min, then freeze-dried and reconstituted with 0.1% formic acid (FA), and finally combined into 10 parts.

MS analysis

The peptides were separated by Easy-nLC (Thermo Fisher Scientific) and then analyzed using a Fusion Lumos Mass Spectrometer (Thermo Fisher Scientific). Each sample was loaded onto the C18-RP analytical column (Thermo Fisher Scientific, Acclaim PepMap RSLC 50 µm × 15 cm, nano viper, P/N164943) in buffer A (0.1% Formic acid) and separated with a linear gradient of buffer B (80% acetonitrile and 0.1% Formic acid) at a flow rate of 300 nL/min for 95 minutes. The linear gradient was as follows: 3% buffer B for 1 min, then 3–18% for 30 min, 18–40% for 44 min, 40–60% for 6 min, 60–100% for 1 min, and held constant at 100% buffer B for 8.5 min and then back to 1% buffer B for 4 min. MS settings included positive ion mode, the MS1 scan (350–1,500 m/z, 120,000 resolution, 5e5 AGC and 50 ms maximal ion time), and 10 data-dependent MS2 scans (200 m/z, 30,000 resolution, 5e4 AGC, 50 ms maximal ion time, HCD, 2.2 m/z isolation window). Ions with a charge state between 2 and 7 were selected. The dynamic exclusion was 60 s, the microscans were 1, and the normalized collision energy was 32%, 37%, and 42%.

Protein identification and quantification

MS/MS raw files were processed using MASCOT engine (Matrix Science, London, UK; version 2.6) embedded into Proteome Discoverer 2.2, and searched against the database (Uniprot_HomoSapiens_20386_20180905). The search parameters were as follows: trypsin as the enzyme with a maximum of two missed cleavages permitted. The mass tolerance was set to 10 ppm for precursor ions and 0.05 Da for MS2 fragments. Carbamidomethyl of Cysteine was set as fixed modification and Oxidation (M) and Acetyl (Protein N-term) were specified as dynamic modifications.

Bioinformatics analysis

Functional analysis of Gene Ontology (GO) and Kyoto Encyclopedia of Genes and Genomes (KEGG) annotation and enrichment analysis-DEPs were annotated using the GO and KEGG databases. Further improvement of the annotation and connection between GO terms was carried out by ANNEX.

In order to explore the underlying mechanisms regulating the observed changes in protein expression profiles, five sub-analyses of IPA (QIAGEN, Redwood City, CA, USA) were performed, including Canonical Pathways, Upstream Regulators, Diseases and Functions, Regulatory effects, and Molecular network analysis.

Statistical analysis

For protein identification, the results were filtered based on a peptide and protein false discovery rate (FDR) ≤1%. Fold change >1.2 or <0.83 with a P value <0.05 (Student's *t*-test) were used to identify differentially-expressed proteins. For GO analysis, fisher's exact test (P value) with BH correction for multiple testing (BH FDR) was used to compare the number of differentially-expressed proteins and total proteins correlated to GO terms or pathways. P<0.05 and FDR <20% or lower were considered statistically significant. Two statistics were used in the IPA analysis. The P value was calculated using a right-tailed Fisher's exact test, which reflects the likelihood that the association or overlap between the DEPs and a given process/pathway is due to random chance. P<0.05 was considered statistically significant. Also, the Z-score was applied in Canonical Pathways, Upstream Regulators, Diseases and Functions, and Regulatory effects analyses to provide predictions on directional effect, with Z-scores greater than 2 or less than –2 being considered as significantly activated or inhibited, respectively.

Results

Table 1 shows the characteristics of hypospadias cases and unaffected controls included in this analysis. The average ages of control and hypospadias group boys were 32.6 and 28 months, respectively, and the difference was not

Table 1 Clinical characteristics of subjects at the time of surgery

Group	Patient ID	Age at surgery (months)	Urethral opening location
Health controls (N=5)	B1	25	Normal
	B2	28	Normal
	B3	30	Normal
	B4	42	Normal
	B5	38	Normal
Severe hypospadias (N=5)	A1	26	Penoscrotal
	A2	30	Scrotal
	A3	20	Penoscrotal
	A4	18	Proximal penile
	A5	46	Perineal

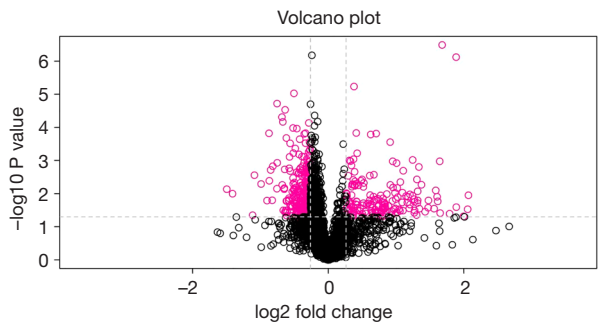

Figure 1 Volcano plot of differentially-expressed proteins in severe hypospadias compared to the unaffected controls. The x-axis is the log2 fold change and y-axis is the –log10 (P value). The vertical dot lines highlight the fold changes of –2 and +2; the horizontal dot line represents a P value of 0.05; the left red circles represent the down-regulated proteins; and the right red circles represent up-regulated proteins.

statistically significant. The distribution of hypospadias categories was as follows: one proximal penile, two penoscrotal, one scrotal, and one perineal, which were all accompanied by chordee.

Differentially expressed proteins between healthy controls and severe hypospadias subjects

Using the TMT proteomic method, a total of 274,366 spectra were obtained, 52,572 of which were matched with the peptide spectrum. In total, 33,395 unique peptides and 5,270 proteins were identified. Compared with the unaffected controls, 299 proteins were down-regulated and 176 proteins were up-regulated in severe hypospadias foreskin tissues. The complete proteins were identified and the expressions (compared to the controls) are provided in supplementary file (https://cdn.amegroups.cn/static/public/TAU-22-155-1.xlsx). The volcano plot showing the distribution of DEPs is shown in *Figure 1*. The top 20 up- and down-regulated DEPs are listed in *Table 2*.

GO annotation and enrichment analysis of DEPs

According to the GO enrichment analysis, the top three molecular functions were associated with chemokine activity, serine-type endopeptidase activity, and antigen and heparin binding. For the cellular component, most DEPs were found in the extracellular space. The biological pathways of DEPs were predominantly related to regulation of complement activation, complement activation and classical pathway molecular function, and blood coagulation (*Figure 2*). As shown in *Figure 3*, the KEGG pathway analysis also verified that DEPs were significantly enriched in pathways associated with complement and coagulation cascades (P=7.95E-21, FDR =1).

IPA-enriched canonical pathways

The canonical pathway analysis identified pathways that were significantly enriched in the DEP dataset. A total of 67 enriched canonical pathways were identified by applying the –log (P value) >2 threshold. Of these 67 representative pathways, the top 20 were ranked according to

Table 2 The top 20 upregulated and downregulated proteins in severe hypospadias patients compared with healthy controls

Gene name	Description	Fold change	P value
Up-regulated proteins			
IGHV3-74	Immunoglobulin heavy variable 3–74	4.19	0.011156
ELANE	Neutrophil elastase	4.15	0.029377
CAMP	Cathelicidin antimicrobial peptide	3.99	0.047796
IGLV2-8	Immunoglobulin lambda variable 2–8	3.70	0.025526
FGG	Fibrinogen gamma chain	3.69	0.000001
APOC1	Apolipoprotein C-I	3.46	0.039973
FGB	Fibrinogen beta chain	3.20	0.000000
S100A12	Protein S100-A12	3.14	0.038598
FGA	Fibrinogen alpha chain	3.13	0.001046
IGHV3-23	Immunoglobulin heavy variable 3–23	3.06	0.017079
PF4	Platelet factor 4	3.04	0.012423
GP1BB	Platelet glycoprotein Ib beta chain	3.00	0.007968
IGHV3-49	Immunoglobulin heavy variable 3–49	2.95	0.028270
EPB42	Erythrocyte membrane protein band 4.2	2.78	0.015971
GYPA	Glycophorin-A	2.78	0.026578
HP	Haptoglobin	2.69	0.034979
ITGA2B	Integrin alpha-IIb	2.59	0.005386
STX19	Syntaxin-19	2.54	0.028154
ZNF648	Zinc finger protein 648	2.53	0.001558
PPBP	Platelet basic protein	2.49	0.008485
Down-regulated proteins			
HLA-DRB1	HLA class II histocompatibility antigen, DRB1-15 beta chain	0.35	0.007260
HLA-A	HLA class I histocompatibility antigen, A-24 alpha chain	0.38	0.010008
ADH1B	Alcohol dehydrogenase 1B	0.46	0.044350
CRABP1	Cellular retinoic acid-binding protein 1	0.47	0.002762
	Immunoglobulin delta heavy chain	0.50	0.005102
SFRP2	Secreted frizzled-related protein 2	0.54	0.016133
GTF2F1	General transcription factor IIF subunit 1	0.55	0.000150
CES1	Liver carboxylesterase 1	0.55	0.004086
LOR	Loricrin	0.56	0.001912
SCIN	Adseverin	0.56	0.015756
LGMN	Legumain	0.57	0.001472

Table 2 (*continued*)

Table 2 (*continued*)

Gene name	Description	Fold change	P value
CRYM	Ketimine reductase mu-crystallin	0.59	0.007077
CYP1B1	Cytochrome P450 1B1	0.59	0.000019
HNMT	Histamine N-methyltransferase	0.59	0.001169
SPON1	Spondin-1	0.62	0.000049
KRT80	Keratin, type II cytoskeletal 80	0.62	0.005411
RNF185	E3 ubiquitin-protein ligase RNF185	0.63	0.000068
LDB3	LIM domain-binding protein 3	0.63	0.031643
CHCHD2	Coiled-coil-helix-coiled-coil-helix domain-containing protein 2	0.64	0.007271
PLD3	Phospholipase D3	0.64	0.006775

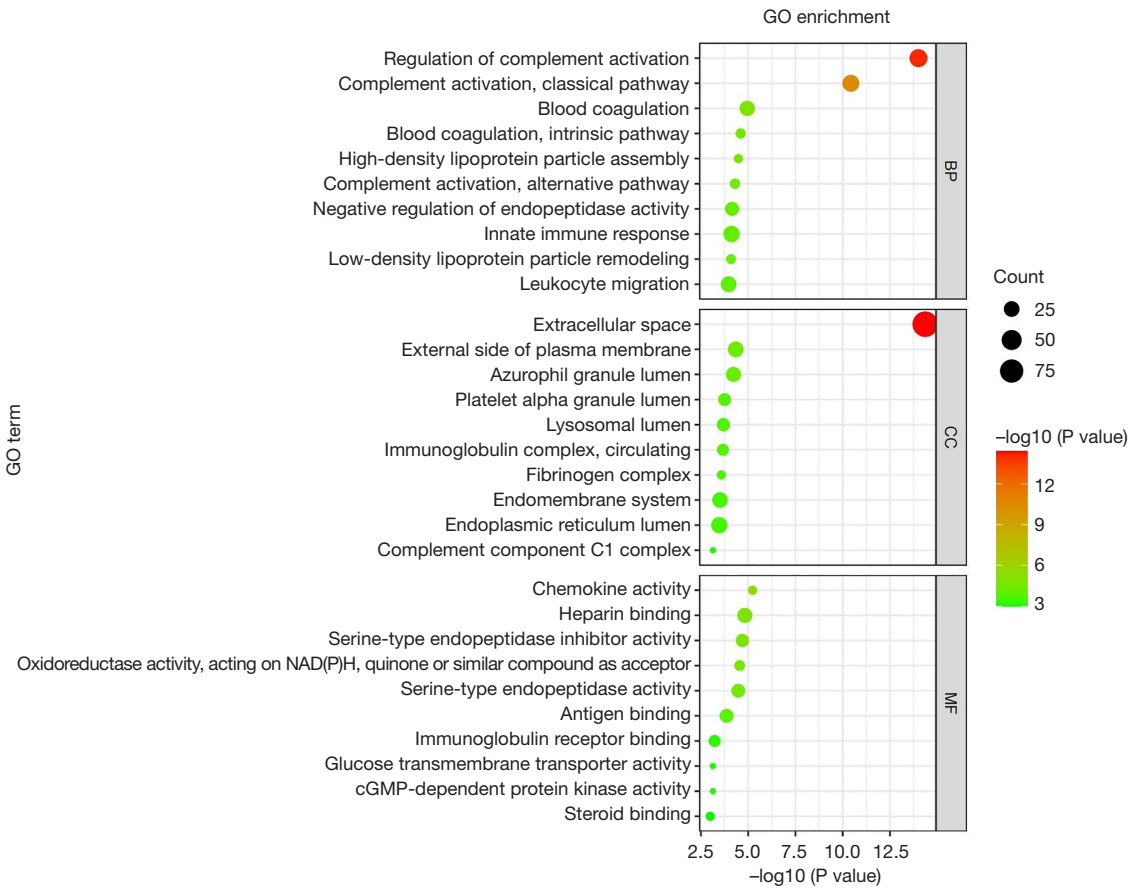

Figure 2 The top 10 most significant GO terms (P<0.05) in DEPs. The dot size represents the number of significant proteins and the color indicates the P value. GO, Gene Ontology; DEP, different expression of protein; BP, biological process; CC, cellular component; MF, molecular function.

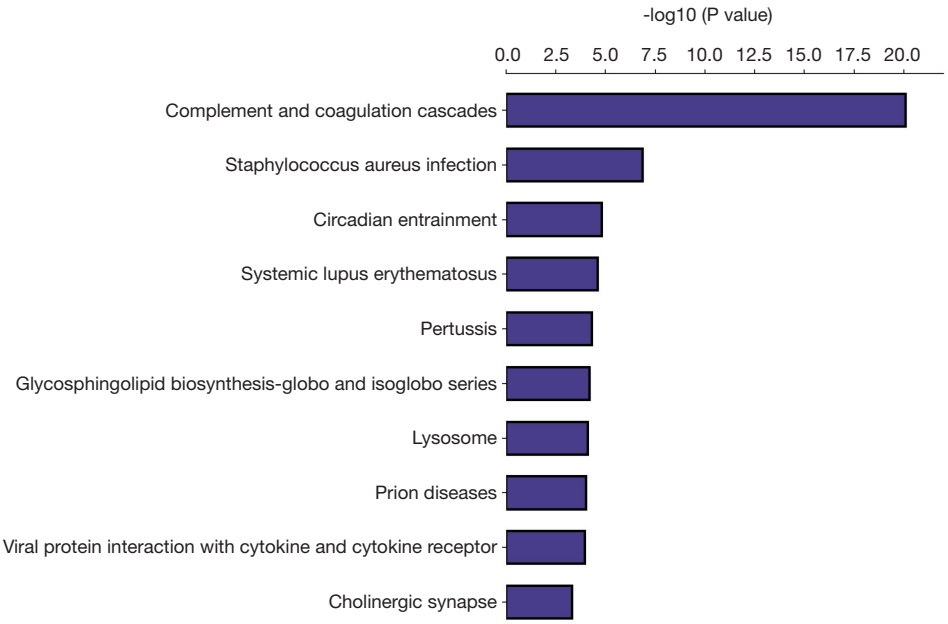

Figure 3 KEGG pathway enrichment analysis of the changed proteins. KEGG, Kyoto Encyclopedia of Genes and Genomes.

their –log (P value), as shown in *Figure 4*, along with the ratio of enriched DEPs to all proteins within each of these signaling pathways. The top five most predicted statistically significant canonical pathways by P value were as follows: "Acute Phase Response Signaling" [–log (P value) =22.5, Z-score =2.673]; "Complement System" [–log (P value) =20.5, Z-score =0.775]; "Coagulation System" [–log (P value) =14.6, Z-score =1.604]; "Extrinsic Prothrombin Activation Pathway [–log (P value) =11.3, Z-score =2.53]"; and "LXR/RXR activation [–log (P value) =10.3, Z-score =3.771]" (*Figure 4*). Fibrinogen alpha chains (FGA) and fibrinogen beta chain (FGB) were the shared DEPs of "Acute Phase Response Signaling", "Coagulation System", and "Extrinsic Prothrombin Activation Pathway".

Downstream functions, upstream regulators and regulatory effects analysis

Diseases-and-functions analysis identifies downstream biological processes and functions that are likely to be causally affected by DEPs, and predicts the directional change on that effect. As shown in *Figure 5*, a large number or biological processes were predicted to be increased in hypospadias patients, especially those in the categories of molecular transport, cell-to-cell signaling and interaction, cellular compromise, hematological system development and function, immune cell trafficking, cellular compromise, and inflammatory response. Among these categories, the specifically increased functions were molecule secretion (Z-score =3.307), granulocyte activation (Z-score =3.071), cell degranulation (Z-score =3.056), myeloid cell degranulation (Z-score =2.934), and phagocyte degranulation (Z-score =2.931). Thirty-five DEPs were involved in the molecule secretion function, including CREB1, APOE, ELANE, FGA, FGB, and FN1 (*Figure 6*), which were up-regulated in the dataset and therefore predicted to increase the molecule secretion function.

Upstream regulator analysis infers upstream regulators that may be responsible for the expression changes observed in the DEP dataset and the directional state of the regulators. By applying the P value of overlap <0.05 threshold, the top-predicted activated regulator was found to be transcription regulator HNF1A (activation Z score =3.175). Other transcription regulators, such as GATA1 (activation Z score =2.929), Jnk (activation Z score =2.791), STAT1 (activation Z score =2.789), and STAT3 (activation Z score =2.646), were also predicted to be significantly activated. Transcription regulator transcription factor EB (TFEB) was revealed to be the most powerful inhibitor (activation Z-score =–2.6).

Regulatory effect analysis was performed to integrate

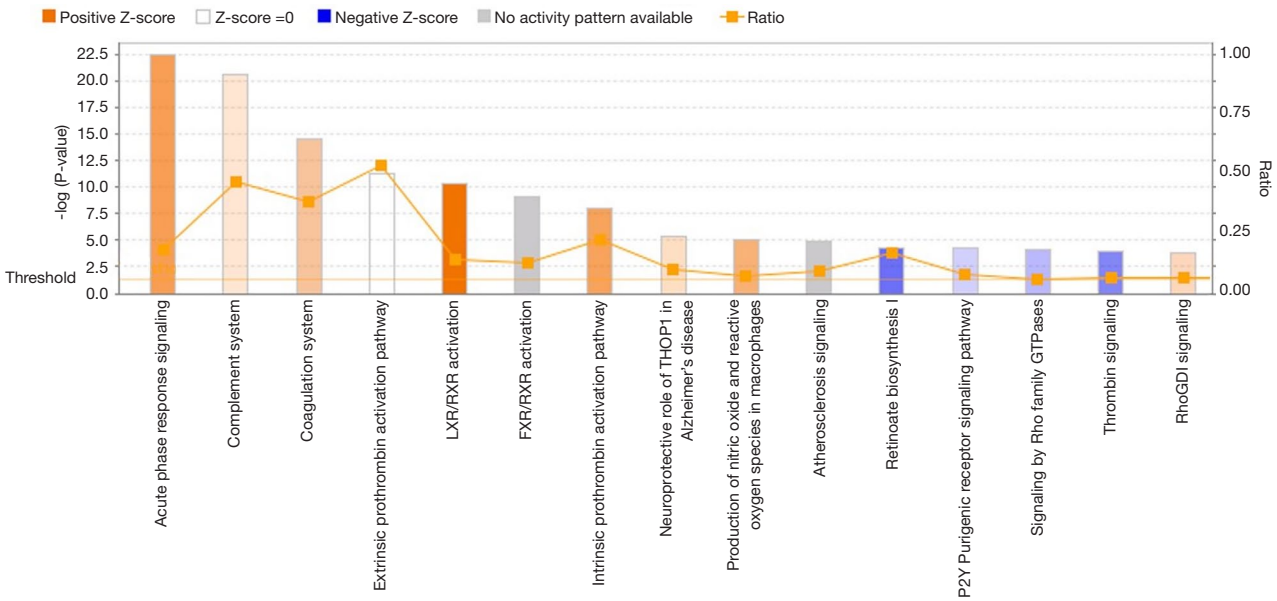

Figure 4 The top 15 canonical pathways enriched in severe hypospadias patients compared with controls. The bar-chart color indicates the predicted directionality activation or inhibition. The left y-axis displayed the –log of Fischer's exact test P value. The right y-axis displayed the ratio of the number of genes derived from the DEP dataset divided by the total number of genes in the pathway. DEP, different expression of protein.

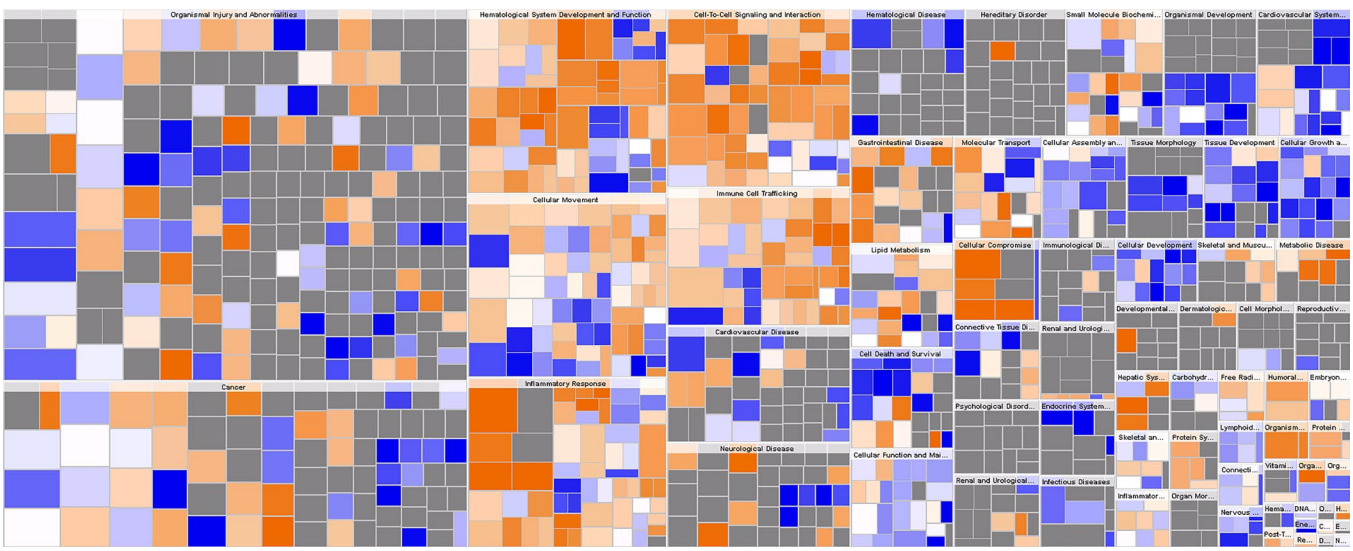

Figure 5 Diseases-and-functions analysis results. Each box represents a biological process or disease. The size of the box represents gene enrichment, and the color of the box indicates the predicted increase or decrease.

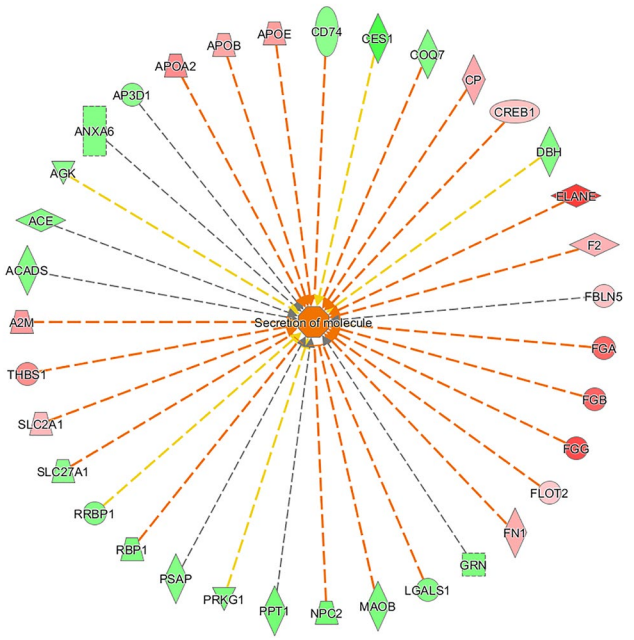

Figure 6 Thirty-five DEPs were involved in the molecule secretion function, including CREB1, APOE, ELANE, FGA, FGB and FN1. DEP, different expression of protein.

the predicted upstream regulator results with downstream effects results and identify how the upstream regulator drive the predicted downstream effects on biological and disease processes that involved the DEPs. We identified a total of 17 types of regulatory effects. Among them, the highest ranked regulatory effect had a consistency score of 5.756, which strongly suggested that CSF1, Jnk, STAT1, and STAT3 may be involved in the activation of myeloid cell degranulation, phagocyte degranulation, and molecule secretion, mainly by mediating their targeted proteins including A2M, APOE, C4A/C4B, C5, CAT, CD74, CFP, CREB1, CTSB, FGA, FGB, FGG, FN1, FOS, HP, LYZ, PF4, RBP1, S100A12, SERPINA3, SLC2A1, and THBS1 (*Figure* 7).

Molecular network analysis

Interaction network analysis shows the interactions between the DEPs in the dataset. All of the networks were then sorted using the score values. The highest ranked network (score 48) was found to mainly affect 'Cell Morphology, Cellular Movement, Connective Tissue Development and

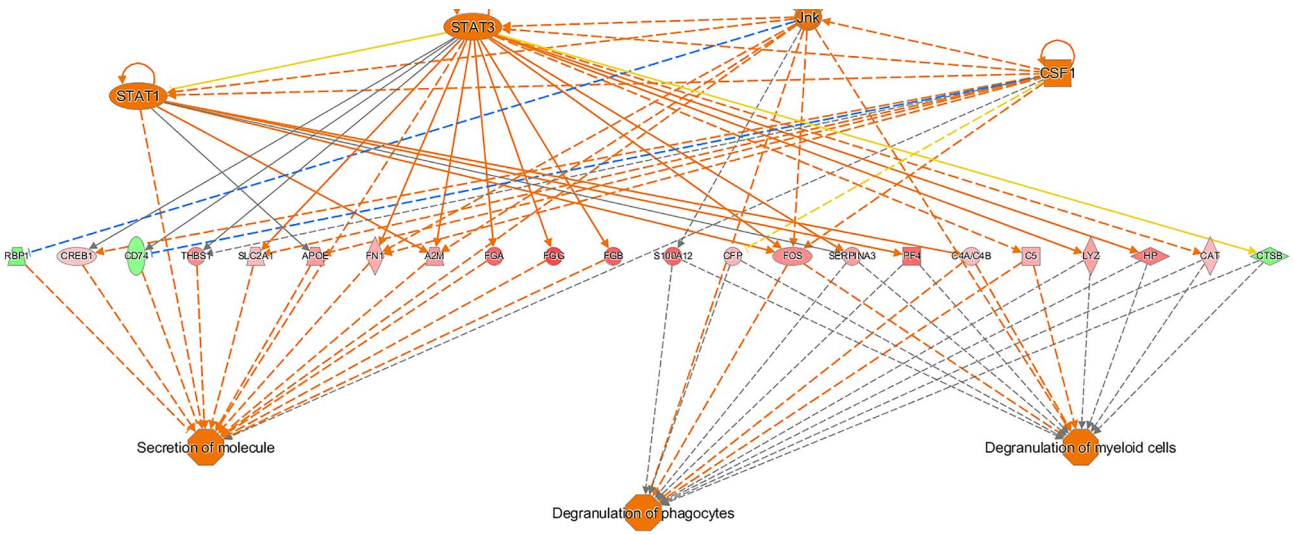

Figure 7 The highest ranked regulatory effect analysis. CSF1, Jnk, STAT1, and STAT3 may be involved in myeloid cell degranulation, phagocyte degranulation, and molecule secretion, mainly via mediating their targeted proteins, including A2M, APOE, C4A/C4B, C5, CAT, CD74, CFP, CREB1, CTSB, FGA, FGB, FGG, FN1, FOS, HP, LYZ, PF4, RBP1, S100A12, SERPINA3, SLC2A1, and THBS1.

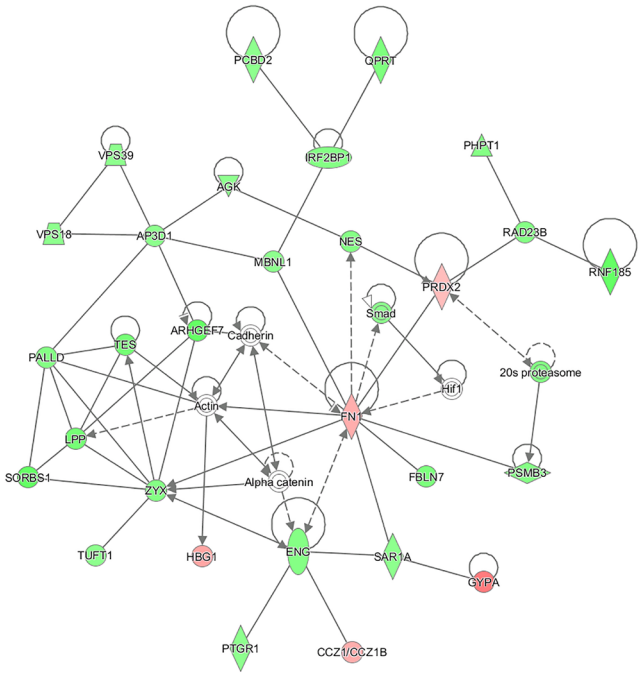

Figure 8 The most significant interaction network between the DEPs. DEP, different expression of protein.

Function', involving proteins such as *20s proteasome*, *Actin*, *AGK*, *alpha-catenin*, *AP3D1*, *ARHGEF7*, *Cadherin*, *CCZ1/CCZ1B*, *ENG*, *FBLN7*, *FN1*, *GYPA*, *HBG1*, *Hif1*, *IRF2BP1*, *LPP*, *MBNL1*, *NES*, *PALLD*, *PCBD2*, *PHPT1*, *PRDX2*, *PSMB3*, *PTGR1*, *QPRT*, *RAD23B*, *RNF185*, *SAR1A*, *Smad*, *SORBS1*, *TES*, *TUFT1*, *VPS18*, *VPS39*, and *ZYX*. The associated interaction network map based on these molecules is shown in *Figure 8*.

Discussion

The clinical characteristics of hypospadias are significantly heterogeneous and complex (17). According to the anatomical location of urethral meatus at the point of medial-ventral side of the penis after chordee has been released, the hypospadias is classified as anterior hypospadias (glanular and subcoronal), middle hypospadias (from distal penile to midshaft) and posterior hypospadias (proximal penile, penoscrotal, scrotal and perineal) (18). Posterior hypospadias is considered as sever hypospadias. The etiology is believed to be multifactorial and heterogeneous by severity (19). Single nucleotide polymorphism (SNP) rs5919436 in the *AR* gene (20), two SNPs in the *STARD3* gene (21), mRNA and protein expression levels of the zinc finger oestrogen-box binding homeobox 1 (*ZEB1*) gene (22), CAG repeats (23), SNP rs17268974 in the steroid sulfatase (*STS*) gene and the diacylglycerol kinase kappa (*DGKK*) gene were found to have severity-dependent correlations (21).

In this study, we analyzed preputial samples from severe hypospadias cases and unaffected controls using a tandem mass tag-labeled quantitative, proteomics approach.

Tandem Mass Tag is a peptides labeling technique where peptide N-terminus and side chain amines are covalently labeled with tags of different masses. A notable advantage of Tandem Mass Tag approach is that the current multiplexing capacity can accommodate up to 16 samples simultaneously. All samples are pooled and further processed together, thus reducing technical variation in the experimental workflow. The multiplexing manner greatly reduces the number of missing peptide quantification values in each TMT experiment and enables achieving deep proteome coverage for multiple samples in a reasonable amount of measurement time. Experimental design, sample preparation and separation, MS acquisition parameters, and data analysis are the key steps to achieve accurate and precise quantitative measurements (24).

Using this approach, we found that compared to the controls, 299 proteins were found to be down-regulated and 176 proteins were found to be up-regulated in severe hypospadias. Functional annotation revealed that these DEPs were mainly in the extracellular space and were associated with complement activation. KEGG analysis showed that the DEPs were significantly enriched in the pathways associated with complement and coagulation cascades. Similarly, the IPA core analysis revealed the enriched pathways of acute phase response signaling and complement system, showing that CSF1, JNK, STAT1, and STAT3 may be involved in the activation of myeloid cell degranulation, phagocyte degranulation, and molecule secretion, mainly by mediating their targeted differentiated expressed proteins, including A2M, APOE, C4A/C4B, C5, CAT, CD74, CFP, CREB1, CTSB, FGA, FGB, FGG, FN1, FOS, HP, LYZ, PF4, RBP1, S100A12, SERPINA3, SLC2A1, and THBS1. HNF-1α was also predicted to be the most activated upstream regulator based on the DEP datasets, linking to the overexpression of FGA, FGB, FN1, C4BPA, APOB, APOA, and SERPING.

In terms of normal urogenital development, the mesoderm, ectoderm and endoderm develop into erectile tissue and stroma, glans penis and skin, and urethral epithelium respectively (4,25). In hypospadias cases, urethral development is abnormal and is usually

characterized by intensified penile curvature and the presence of central fibrous bands on the corpus cavernosum penis (26). Anatomical studies have shown that, compared with normal penile specimens, the urethral plate of hypospadiac specimens is well vascularized, has a rich nerve supply, as well as an extensive muscular and connective tissue backing. The extensive blood vessels, glandular structure, and muscles under the urethral plate correspond to an abnormally-formed corpus spongiosum and suggest an abortive attempt at urethral formation in hypospadias (27,28). Additionally, Nozohoor *et al.* provided histological evidence showing that hypospadias had a distinct anatomic pathology, consisting of fibrovascular tissue with coverage of squamous epithelium and urothelial pits, in which inflammatory cells are a recurrent feature (29). Hypocellular fibrous tissue with moderate to rich vascularity were found in hypospadias urethral plate biopsies, with sparse bundles of smooth muscle cells crossing through the stroma along with sparse nerve bundles. Hayashi *et al.* reported the presence of collagen subtype I in all areas of the excised tissue, while collagen subtype III was not detected, which implied that the tissue beneath the urethral plate did not form distensible elastic tissues (30).

In our study, expression of the neutrophil elastases (NE/ELANE) protein was observed to be four times higher in hypospadias tissues compared to unaffected control. ELANE form a subfamily of serine proteases that are capable of hydrolyzing essentially all of the extracellular matrix (ECM) proteins, including collagens (types I–III), type IV collagen, entactin, fibronectin, laminin, and elastin (31,32). It has also been suggested to play a role in degenerative and inflammatory diseases. *In vitro* assays have shown that ELANE induces fibroblast proliferation and myofibroblast differentiation through PI3K hyperactivity. Neutrophil elastases knockout mice are protected from asbestos-induced lung fibrosis, displaying reduced fibroblast and myofibroblast content when compared with controls (33). Elastase inhibition decreases scar formation after spinal cord injury (34).

Fibronectin-1 FN1, fibrinogen alpha beta and gamma chain FGA, FGB, and FGG were also found to be upregulated in hypospadias patients. During injury, infection, and inflammation, FGA, FGG, and FGB are cleaved by the protease thrombin to yield monomers and polymerize to form insoluble fibrin matrix, thereby stimulating monocyte infiltration and rapid differentiation into macrophages. Activated macrophages promote angiogenesis and stimulate fibroblast migration and proliferation (35), which begin to synthesize and deposit large quantities of ECM proteins, including collagen type I and III, and FN. In case of compromised feedback mechanisms, continuous ECM synthesis, deposition, and remodeling ensue, and myofibroblasts remain. Enhanced chronic vascular remodeling and ECM crosslinking eventually leads to aberrant fibrosis (36). Fibrinogens are transcriptionally upregulated by IL-6 during the acute-phase of the inflammatory response to help restore homeostasis and restrict proteolytic and/or fibrogenic activity and tissue damage (37). FN1 has been indicated to play a crucial role in mediating cell attachment and function, as well as in cell migration during development (38).

Additionally, we observed that the expression of the proto-oncogene, c-Fos protein FOS, was 2.5 times higher in our hypospadias group. C-Fos expression has been increasingly used as a reflection of neuronal activation. In a recent study, Xiang *et al.* found that c-Fos protein levels were higher in the genital tubercle of di(2-ethylhexyl) phthalate (DEHP)-induced rats than that in control rats. Compared to controls, hypospadias group showed significant higher C-Fos mRNA and protein levels, and c-Fos protein levels were markedly higher in the severe hypospadias group compared to the mild hypospadias group (39). C-Fos is also involved in the downstream JNK pathway signaling to promote cell apoptosis (40). Piñeyro-Ruiz *et al.* also revealed apoptotic signaling pathways during the development of mild hypospadias (16). JNK has been proposed to be associated with mesenchymal cell migration in the process of external male genitalia defect development. Li *et al.* reported that JNK protein levels were significantly increased in mild or severe hypospadias subjects compared to the controls, and hypospadias group had increased phosphorylation JNK1 and JNK2 protein expression in the mesenchymal cell layers of the preputial subcutaneous mesenchymal cell layer (17).

Further support of the involvement of inflammation and fibrosis in the development of severe hypospadias is evidenced by two predicted upstream regulators, STAT3 and HNF-1α. HNF-1α has been shown to coordinates the interaction of STAT3/IL-6 and c-Fos, leading to synergistic transcriptional upregulation of promoters such as fibrinogen promoters. The HNF-1/c-Fos and HNF-1/STAT3 protein complexes have been detected in mouse cell lines overexpressing STAT3/c-Fos/HNF-1 (41). In addition, expression profiling and functional studies *in vitro* and *in vivo* have demonstrated that STAT3 activation is mediated by the combined action of JAK, SRC, c-ABL, and

JNK kinases. Fibroblast-specific knockout of STAT3 or its pharmacological inhibition have been shown to ameliorate skin fibrosis in experimental mouse models. Thus, STAT3 integrates several profibrotic signals and might be a core mediator of fibrosis (42).

Conclusions

To the best of our knowledge, this is the first study investigating the protein expression changes between severe hypospadias and unaffected controls. Our findings raise questions regarding the role of inflammatory activity in the pathology of severe hypospadias. This approach highlights the possibility of using non-surgical approaches to limit fibrotic signals and function, which is a promising potential therapeutic strategy for hypospadias patients.

Acknowledgments

Funding: This study was funded by the Science and Technology Projects in Guangzhou (No. 202102020097), the Guangzhou institute of Pediatrics/Guangzhou Women and Children's Medical Center (Nos. pre-NSFC-2018-016, YIP-2018-021, GWCMC2020-4-009), and the Natural Science Foundation of Guangdong Province, China (No. 2019A1515011178).

Footnote

Reporting Checklist: The authors have completed the MDAR reporting checklist. Available at https://tau.amegroups.com/article/view/10.21037/tau-22-155/rc

Data Sharing Statement: Available at https://tau.amegroups.com/article/view/10.21037/tau-22-155/dss

Conflicts of Interest: All authors have completed the ICMJE uniform disclosure form (available at https://tau.amegroups.com/article/view/10.21037/tau-22-155/coif). The authors have no conflicts of interest to declare.

Ethical Statement: The authors are accountable for all aspects of the work in ensuring that questions related to the accuracy or integrity of any part of the work are appropriately investigated and resolved. This study protocol was approved by the Ethics Committee of Guangzhou Women and Children's Medical Center, Guangdong, China (No. GWCMC-2020201), and was carried out in accordance with all relevant guidelines and regulations. Written informed consent was obtained from all patients or their parental/legal guardians. The study was conducted in accordance with the Declaration of Helsinki (as revised in 2013).

References

1. Ságodi L, Kiss A, Kiss-Tóth E, et al. Prevalence and possible causes of hypospadias. Orv Hetil 2014;155:978-85.
2. Springer A, van den Heijkant M, Baumann S. Worldwide prevalence of hypospadias. J Pediatr Urol 2016;12:152.e1-7.
3. Thorup J, Nordenskjöld A, Hutson JM. Genetic and environmental origins of hypospadias. Curr Opin Endocrinol Diabetes Obes 2014;21:227-32.
4. Richard MA, Sok P, Canon S, et al. Altered mechanisms of genital development identified through integration of DNA methylation and genomic measures in hypospadias. Sci Rep 2020;10:12715.
5. Bouty A, Ayers KL, Pask A, et al. The Genetic and Environmental Factors Underlying Hypospadias. Sex Dev 2015;9:239-59.
6. Carmichael SL, Witte JS, Ma C, et al. Hypospadias and variants in genes related to sex hormone biosynthesis and metabolism. Andrology 2014;2:130-7.
7. Xie H, Lin XL, Zhang S, et al. Association between diacylglycerol kinase kappa variants and hypospadias susceptibility in a Han Chinese population. Asian J Androl 2018;20:85-9.
8. Karabulut R, Turkyilmaz Z, Sonmez K, et al. Twenty-Four Genes are Upregulated in Patients with Hypospadias. Balkan J Med Genet 2013;16:39-44.
9. Chen T, Li Q, Xu J, et al. Mutation screening of BMP4, BMP7, HOXA4 and HOXB6 genes in Chinese patients with hypospadias. Eur J Hum Genet 2007;15:23-8.
10. Carmichael SL, Shaw GM, Lammer EJ. Environmental and genetic contributors to hypospadias: a review of the

epidemiologic evidence. Birth Defects Res A Clin Mol Teratol 2012;94:499-510.
11. Fredell L, Kockum I, Hansson E, et al. Heredity of hypospadias and the significance of low birth weight. J Urol 2002;167:1423-7.
12. Huisma F, Thomas M, Armstrong L. Severe hypospadias and its association with maternal-placental factors. Am J Med Genet A 2013;161A:2183-7.
13. Baskin LS. Hypospadias and urethral development. J Urol 2000;163:951-6.
14. Bonde JP, Flachs EM, Rimborg S, et al. The epidemiologic evidence linking prenatal and postnatal exposure to endocrine disrupting chemicals with male reproductive disorders: a systematic review and meta-analysis. Hum Reprod Update 2016;23:104-25.
15. Chen L, Wang J, Lu W, et al. Characterization With Gene Mutations in Han Chinese Patients With Hypospadias and Function Analysis of a Novel AR Genevariant. Front Genet 2021;12:673732.
16. Piñeyro-Ruiz C, Serrano H, Jorge I, et al. A Proteomics Signature of Mild Hypospadias: A Pilot Study. Front Pediatr 2020;8:586287.
17. Li M, Qiu L, Lin T, et al. c-Jun N-terminal kinase is upregulated in patients with hypospadias. Urology 2013;81:178-83.
18. Sheldon CA, Duckett JW. Hypospadias. Pediatr Clin North Am 1987;34:1259-72.
19. Piñeyro-Ruiz C, Serrano H, Pérez-Brayfield MR, et al. New frontiers on the molecular underpinnings of hypospadias according to severity. Arab J Urol 2020;18:257-66.
20. Adamovic T, Thai HT, Liedén A, et al. Association of a tagging single nucleotide polymorphism in the androgen receptor gene region with susceptibility to severe hypospadias in a Caucasian population. Sex Dev 2013;7:173-9.
21. Singh N, Gupta DK, Sharma S, et al. Single-nucleotide and copy-number variance related to severity of hypospadias. Pediatr Surg Int 2018;34:991-1008.
22. Qiao L, Tasian GE, Zhang H, et al. Androgen receptor is overexpressed in boys with severe hypospadias, and ZEB1 regulates androgen receptor expression in human foreskin cells. Pediatr Res 2012;71:393-8.
23. Parada-Bustamante A, Lardone MC, Madariaga M, et al. Androgen receptor CAG and GGN polymorphisms in boys with isolated hypospadias. J Pediatr Endocrinol Metab 2012;25:157-62.
24. Zecha J, Satpathy S, Kanashova T, et al. TMT Labeling for the Masses: A Robust and Cost-efficient, In-solution Labeling Approach. Mol Cell Proteomics 2019;18:1468-78.
25. Baskin L, Shen J, Sinclair A, et al. Development of the human penis and clitoris. Differentiation 2018;103:74-85.
26. Baskin LS, Ebbers MB. Hypospadias: anatomy, etiology, and technique. J Pediatr Surg 2006;41:463-72.
27. Erol A, Baskin LS, Li YW, et al. Anatomical studies of the urethral plate: why preservation of the urethral plate is important in hypospadias repair. BJU Int 2000;85:728-34.
28. Snodgrass W, Patterson K, Plaire JC, et al. Histology of the urethral plate: implications for hypospadias repair. J Urol 2000;164:988-9; discussion 989-90.
29. Nozohoor Ekmark A, Grelaud D, Hansson E, et al. The Cellular Architectures of Hypospadias. Pediatr Dev Pathol 2020;23:476-8.
30. Hayashi Y, Mizuno K, Kojima Y, et al. Characterization of the urethral plate and the underlying tissue defined by expression of collagen subtypes and microarchitecture in hypospadias. Int J Urol 2011;18:317-22.
31. Gregory AD, Kliment CR, Metz HE, et al. Neutrophil elastase promotes myofibroblast differentiation in lung fibrosis. J Leukoc Biol 2015;98:143-52.
32. Hedstrom L. Serine protease mechanism and specificity. Chem Rev 2002;102:4501-24.
33. Jin Z, Sun J, Song Z, et al. Neutrophil extracellular traps promote scar formation in post-epidural fibrosis. NPJ Regen Med 2020;5:19.
34. Kumar H, Choi H, Jo MJ, et al. Neutrophil elastase inhibition effectively rescued angiopoietin-1 decrease and inhibits glial scar after spinal cord injury. Acta Neuropathol Commun 2018;6:73.
35. Schultz GS, Wysocki A. Interactions between extracellular matrix and growth factors in wound healing. Wound Repair Regen 2009;17:153-62.
36. Kisseleva T, Brenner DA. Mechanisms of fibrogenesis. Exp Biol Med (Maywood) 2008;233:109-22.
37. Moshage H. Cytokines and the hepatic acute phase response. J Pathol 1997;181:257-66.
38. Frantz C, Stewart KM, Weaver VM. The extracellular matrix at a glance. J Cell Sci 2010;123:4195-200.
39. Xiang H, Wang S, Kong X, et al. c-Fos is upregulated in the genital tubercle of DEHP-induced hypospadiac rats and the prepuce of patients with hypospadias. Syst Biol Reprod Med 2021;67:193-200.
40. Johnson GL, Nakamura K. The c-jun kinase/stress-activated pathway: regulation, function and role in human disease. Biochim Biophys Acta 2007;1773:1341-8.
41. Leu JI, Crissey MA, Leu JP, et al. Interleukin-6-induced STAT3 and AP-1 amplify hepatocyte nuclear factor

1-mediated transactivation of hepatic genes, an adaptive response to liver injury. Mol Cell Biol 2001;21:414-24.
42. Chakraborty D, Šumová B, Mallano T, et al. Activation of STAT3 integrates common profibrotic pathways to promote fibroblast activation and tissue fibrosis. Nat Commun 2017;8:1130.

(English Language Editor: A. Kassem)

Cite this article as: Zhu S, Fu W, Hu J, Tang X, Cui Y, Jia W. Quantitative proteomics reveals specific protein regulation of severe hypospadias. Transl Androl Urol 2022;11(4):495-508. doi: 10.21037/tau-22-155

